Available online at www.sciencedirect.com
ScienceDirect
Journal of Power Sources 165 (2007) 491–499
JOURNAL OF POWER SOURCES
www.elsevier.com/locate/jpowsour

Review

Review on electrode–electrolyte solution interactions, related to cathode materials for Li-ion batteries

Doron Aurbach [a,*], Boris Markovsky [a], Gregory Salitra [a], Elena Markevich [a], Yossi Talyossef [a], Maxim Koltypin [a], Linda Nazar [b], Brian Ellis [b], Daniella Kovacheva [c]

[a] *Department of Chemistry, Bar-Ilan University, Ramat-Gan 52900, Israel*
[b] *Department of Chemistry, University of Waterloo, Waterloo, Canada*
[c] *IGIC, Bulgarian Academy of Science, Sofia, Bulgaria*

Available online 27 November 2006

Abstract

In this paper we review some critical aspects related to interactions between cathode materials and electrolyte solutions in lithium-ion batteries. Previous results are briefly summarized, together with the presentation of new results. This review deals with the basic anodic stability of commonly-used electrolyte solutions for Li-ion batteries (mostly based on alkyl carbonate solvents). We discuss herein the surface chemistry of the following cathode materials: $LiCoO_2$, V_2O_5, $LiMn_2O_4$, $LiMn_{1.5}Ni_{0.5}O_4$, $LiMn_{0.5}Ni_{0.5}O_2$, and $LiFePO_4$. The methods applied included solution studies by ICP, Raman, X-ray photoelectron and FTIR spectroscopies, and electron microscopy, all in conjunction with electrochemical techniques. General phenomena are the possible dissolution of transition metal ions from these materials, which leads to changes in the active mass and a retardation in the electrode kinetics due to the formation of blocking surface films. These phenomena are significant mostly at elevated temperatures and in electrolyte solutions containing acidic species. Water-contaminated $LiPF_6$ solutions can reach a high concentration of acidic species (e.g., HF), which is detrimental to the performance of materials such as $LiCoO_2$ and $LiFePO_4$. Both $LiMn_{1.5}Ni_{0.5}O_4$ and $LiMn_{0.5}Ni_{0.5}O_2$, even when used as nanomaterials, show a high stability in commonly-used electrolyte solutions at high temperatures. This stability is attributed to unique surface chemistry that is correlated to the presence of Ni ions in the lattice.

Keywords: Cathodes; Surface chemistry; Impedance; Capacity fading; Electrolyte solutions

Contents

1. Introduction

In recent years, rechargeable Li-ion battery systems have become a prominent technology in the global battery market. These batteries offer the highest energy density available to date for rechargeable batteries. While currently produced Li-ion batteries power mostly small devices such as cellular phones, portable computers and mobile electro-optic equipment, intensive world-wide efforts are taking place to push the technology even further to much more demanding applications such as large and fast batteries for electric vehicles.

* Corresponding author. Tel.: +972 3 5318309; fax: +972 5351250.
E-mail address: aurbach@mail.biu.ac.il (D. Aurbach).

0378-7753/$ – see front matter © 2006 Elsevier B.V. All rights reserved.
doi:10.1016/j.jpowsour.2006.10.025

The major factor that determines the energy density, rate capability (i.e., power density), and cost of Li-ion batteries is the cathode. The current predominant cathode material is $LiCoO_2$, which is very expensive, possesses limited practical capacity (<140 mAh g^{-1}) and rates, and suffers from stability problems at elevated temperatures in the common electrolyte solutions (e.g., a $LiPF_6$ salt in a mixture of alkyl carbonate solvents). Consequently, intensive R&D work on new cathode materials for Li-ion batteries is being carried out today by hundreds of research groups throughout the world. The major cathode materials currently being explored are $LiMn_2O_4$ spinel [1], $LiFePO_4$ [2], $LiMn_{1-x-y}Ni_xCo_yO_2$ [3], $LiMn_{0.5}Ni_{0.5}O_2$ [4], $LiMn_{1.5}Ni_{0.5}O_4$ spinel [5], $LiNi_{1-x}MO_2$ (M = a third metal, Co, Al) [6], Li_xVO_y [7], and $Li_xM_yVO_z$ (M = a third metal such as Ca, Cu) [8]. Much attention is given to the development of reliable synthetic routes for these materials, their structural analysis and basic electrochemical behavior. Furthermore, the scientific community studying these cathode materials is reaching a very high level of precision in structural analysis, using synchrotron, X-ray radiation (for *in situ* XRD [9], XANES [10], EXAFS [11]), high resolution electron microscopy/electron diffraction [12], and solid-state NMR [13].

All cathode materials of interest for Li-ion batteries are reactive with the commonly-used electrolyte solutions, thus developing a rich surface chemistry [14]. There is strong evidence that most of the above-mentioned lithiated transition metal oxides are covered by surface films in solutions, due to spontaneous reactions with solution components [15]. Hence, the electrochemical behavior of most cathode materials may depend very strongly on their surface chemistry in solutions and phenomena such as surface film formation. Similar to Li and Li-C anodes, many types of cathodes for Li-ion batteries can also be considered as SEI [16] electrodes (i.e., covered by a Li-ion conducting interphase [16]). There are many possible reactions of Li_xMO_y materials with solutions that contain alkyl carbonate solvents and Li salts such as $LiPF_6$. These include acid–base interactions between the Li_xMO_y and trace HF, which are inevitably present in $LiPF_6$ solutions, nucleophilic attack of the electrophilic alkyl carbonate molecules by oxygen ions on the transition metal oxide, surface-induced polymerization of cyclic alkyl carbonates to polycarbonates, and redox reactions with solution species (both reduction and oxidation processes that may lead to a change in the oxidation state of the transition metal, and to dissolution of transition metal ions into the solution). In contrast to the precision that can be achieved in the bulk analysis of the cathode materials, their rigorous surface analysis is much more difficult, because very thin surface films may be formed whose composition and structure can be profoundly influenced by contaminants in the solutions (even at the ppm level).

This paper describes some recent studies related to the surface chemistry of several cathode materials of interest. These include $LiCoO_2$, $LiMn_{1.5}Ni_{0.5}O_4$, $LiMn_{0.5}Ni_{0.5}O_2$, $Li_xV_2O_5$, and olivines. Surface-sensitive techniques such as FTIR, Raman, XPS, and electron microscopy were used in conjunction with bulk analytical techniques (ICP, XRD) and electrochemical methods (voltammetry, chronopotentiometry, and impedance spectroscopy). The effect of the particles' size on their reactivity (i.e., micro *versus* nano) was also explored.

2. Experimental

The $LiCoO_2$ used was a commercial product (OMG Inc., the particle size was several microns). Microparticulate $LiMn_{1.5}Ni_{0.5}O_4$ was obtained from LG Chem. [17] (spinel structure, particle size of 2–3 μm). Microparticles (several microns in size) of $LiNi_{0.5}M_{0.5}O_2$ were synthesized from LiOH, Mn, and Ni acetates via a solution reaction followed by solid-state/high temperature calcinations step, according to a published procedure [18]. Nanoparticles of $LiNi_{0.5}M_{0.5}O_2$ and $LiMn_{1.5}Ni_{0.5}O_2$ were synthesized by the self-combustion reaction (SCR) modified by Kovacheva and co-workers [19]. Three $LiFePO_4$ olivine compounds were synthesized as summarized below:

1. "Sol–gel" $LiFePO_4$ (denoted as Sample 1) was produced by reacting stoichiometric amounts of Li_3PO_4, H_3PO_4, and $FeC_6H_5O{\cdot}2H_2O$ under flowing argon at 600 °C for 15 h, followed by a treatment under 7% H_2/N_2 at 600 °C for 1 h. The final product contains 3% carbon. Aside from the carbon, the material was phase-pure as determined by XRD: no detectable iron phosphide or other impurities were present.
2. "Solid-state" $LiFePO_4$ (denoted as Sample 2) was produced by ball-milling stoichiometric amounts of $FeC_2O_4{\cdot}2H_2O$, $NH_4H_2PO_4$, and Li_2CO_3, firing the mixture at 600 °C for 12 h, and then again at 700 °C in a flowing 7% H_2N_2 stream. The final product contains 3% C, surface FeP, and/or Fe_2P as determined by a combination of elemental analysis, TGA, and XRD. The contributions of the phosphides were estimated to be <5%
3. "Hydrothermal" $LiFePO_4$ (denoted as Sample 3) was produced by reacting H_3PO_4 and $(NH_4)_2Fe(SO_4)_2$, LiOH, and ascorbic acid in an autoclave (Parr pressure bomb) for 15 h at 190 °C. The solid product was sintered at 600 °C for 6 h under flowing argon. The material contains traces of $Fe_2P_2O_7$ and 1.8% carbon.

Thin film V_2O_5 electrodes were produced by sputtering V_2O_5 from pellets onto inert metal current collectors (e.g., gold foils) by high voltage ionization at high vacuum [20], as well as composite electrodes comprising nanoparticles of V_2O_5. The latter were produced in two stages: the formation of carbon-coated V_2O_3 nanoparticles by the RAPET method [21], followed by heating them in air up to 400 °C, which formed nanoparticles of V_2O_5 partially covered by a thin film of carbon layer [22].

In general, two types of electrodes were studied:

1. Composite electrodes comprising the active mass (≈80% by weight), carbon black, and polyvinylidene difluoride (PVdF) binder (≈10% by weight each) on Al foil current collectors.

2. Binder-free electrodes in which the active mass was embedded by pressure onto Al foil current collectors.

The preparation of the composite electrodes has already been described in detail [23].

The electrolyte solutions used included $LiClO_4$ and $LiPF_6$ 1–1.5 M in mixtures of EC-DMC or EC-EMC (Merck Inc. and Tomiyama Inc., Li battery grade used as received). We also used $LiPF_6$ solutions that were deliberately contaminated by water (up to 800 ppm). The temperature range included 25–80 °C (using the appropriate thermostats). The techniques and instrumentation included: ICP and MicroRaman spectrometer from Jobin-Ivon Inc.; FTIR spectrometer from Nicolet Inc. (Magna 860) in transmittance and reflectance modes; XPS (HS AXIS) from Kratos Inc.; XRD was measured by a Bruker D8 Advance powder diffractometer using standard Bragg-Brentano geometry with Cu Kα radiation (λ = 1.5406 Å). Data were collected from 10 to 70° in 2θ); SEM (JSM-840) from Jeol Inc. and standard electrochemical techniques (voltammetry, EIS, chronopotentiometry) using equipment from Maccor, Arbin, Solatron, and Eco Chemie.

3. Results and discussion

3.1. On the anodic stability of the electrolyte solutions

The intrinsic anodic stability of polar aprotic electrolyte solutions relevant to Li-ion batteries is generally determined by the solvents, and not by the Li salts that are commonly used. It is possible to classify three systems in terms of stability to electrochemical oxidation:

1. Systems containing C–O–C ether linkages, including ethereal solutions or polymer electrolytes based on polyethers (e.g., polyethylene oxide, PEO), and its derivatives. These can be oxidized below 4 V [24] *versus* Li/Li^+ due to the intrinsic limited anodic stability of the ether linkage (i.e., C–O–C bonds).
2. Electrolyte solutions comprising solvents such as organic esters or alkyl carbonates and gel systems containing alkyl carbonates (i.e., polymeric matrices such as PVdF derivatives or poly polyacrylonitrile derivatives that are mixed with Li salts and alkyl carbonate solvents). These seem to have apparent electrochemical windows of more that 4.5–5 V [25].
3. Ionic liquids such as derivatives of imidazolium or pyrrolidinium salts demonstrate high anodic stability, >5 V *versus* Li/Li^+ [26]. There is a growing interest in these systems in relation to Li batteries [27]. However, their applicability for practical use is still very questionable.

Hence, the most important electrolyte systems for Li-ion batteries are the liquid solutions based on alkyl carbonate solvents, which are apparently compatible with high voltage cathode materials (up to 5 V *versus* Li/Li^+ [17]) and enable reasonable performance at low temperatures. However, rigorous studies of the electrochemical behavior of alkyl carbonate-based solutions with metal electrodes, which included the use of *in situ* FTIR spectroscopy and EQCM revealed that alkyl carbonate solvents can be oxidized on platinum and gold electrodes at potentials above 3.5 V (Li/Li^+) [28]. These processes do not form precipitates as proven by EQCM [28]. The products identified by *in situ* FTIR, NMR, and GCMS [28] include CO, CO_2, and organic species with ester, aldehyde, and OH groups. Potentiodynamic studies of these oxidation processes demonstrate that the kinetics are very sluggish up to 4.5 V (Li/Li^+), as only a low current density can be measured. At potentials >4.5 *versus* Li/Li^+, significant oxidation of alkyl carbonates is observed. Since Li-ion batteries operate at potentials up to 5 V and can undergo hundreds of charge–discharge cycles, it is clear that massive oxidation processes of alkyl carbonate solvents are largely inhibited on most (if not all) of the composite positive electrodes used in Li batteries. However, the small-scale oxidation processes of alkyl carbonates at potentials above 3.5 V described above can affect the surface chemistry of the positive electrodes and their possible passivation processes.

3.2. On the surface chemistry of $LiCoO_2$ electrodes

$LiCoO_2$ electrodes have two levels of performance. In standard $LiPF_6$ solutions with a relatively low level of acidic contamination (high ratio between the electrode's active mass and solution volume), $LiCoO_2$ electrodes can be cycled very well at temperatures above 60 °C. On the other hand, in solutions containing acidic contaminants (e.g., HF in $LiPF_6$ solutions, water-contaminated solutions), $LiCoO_2$ can be deactivated as demonstrated in Fig. 1(a and b). Moreover, an examination of full cells cycled at 60 °C comprising a $LiCoO_2$ cathode, an MCMB anode, and $LiPF_6$ based electrolytes clearly showed that the cause of any capacity fading is the MCMB electrode, as demonstrated in Fig. 1c. Binder-free or composite electrodes prepared from $LiCoO_2$ (see above) were stored at 60 °C in EC-DMC solvent mixtures, standard $LiPF_6$ solutions, and water-contaminated $LiPF_6$ solutions containing up to 800 ppm H_2O. The solutions were analyzed by ICP for cobalt-ion content, and the $LiCoO_2$ powders were studied by Raman spectroscopy, XRD, and electron microscopy. The major results are summarized below [29]:

1. We failed to detect Co dissolution in salt-free solvent mixtures.
2. Co dissolution occurs in $LiPF_6$ solutions and is very pronounced in water-contaminated solutions. The temperature strongly affects Co-ion dissolution (which increases as the temperature is raised).
3. Co dissolution is most pronounced from composite electrodes containing $LiCoO_2$ and a PVdF binder. It is very important to note that cobalt-ion dissolution from electrodes comprising $LiCoO_2$ particles embedded in Al foil (no PVdF), or $LiCoO_2$ powder stored in solution (even when containing PVdF powder as well), was much less pronounced than that observed with composite electrodes containing $LiCoO_2$ and PVdF in physical contact.

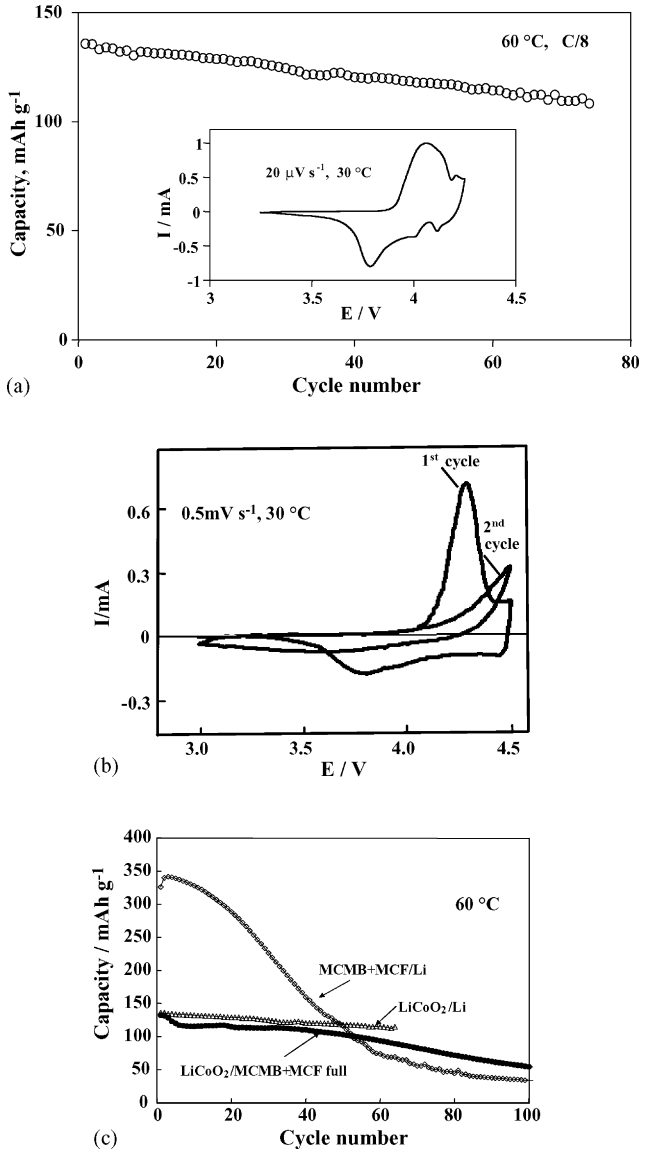

Fig. 1. Cycling behavior and CV of $LiCoO_2$ electrodes: (a) "thick" electrodes (13 mg of $LiCoO_2$ active mass) in coin-type cells (right inset shows CV of the identical electrode), (b) "thin" electrode (1 mg of $LiCoO_2$ active mass) in flooded cell, and (c) full cell $LiCoO_2$/MCMB + MCF and two half cells: MCMB + MCF/Li and $LiCoO_2$/Li at *C*/8. Electrolyte solution composition: 1 M $LiPF_6$ in EC/EMC 1:2.

Fig. 2 shows the Raman spectra of: a pristine $LiCoO_2$ electrode; a $LiCoO_2$ powder after being stored in an EC-DMC/$LiPF_6$ solution that also contains PVdF; an electrode comprising $LiCoO_2$ and Al foil but no PVdF binder; and a composite $LiCoO_2$/carbon black/PVdF/Al electrode after being stored in an EC-DMC/$LiPF_6$ solution at 60 °C. The Raman spectra measured from the $LiCoO_2$ powder or an $LiCoO_2$/Al electrode after storage are very similar to those of the pristine material. However, the Raman spectrum measured from the composite electrodes after storage clearly shows new peaks, which we assign to Co_3O_4 and delithiated CoO_2 (denoted by the arrows in Fig. 2). These results correlate very well with the Co dissolution tests that revealed enhanced Co-ion dissolution from composite electrodes in $LiPF_6$ solutions. Prolonged storage tests at 60 °C also

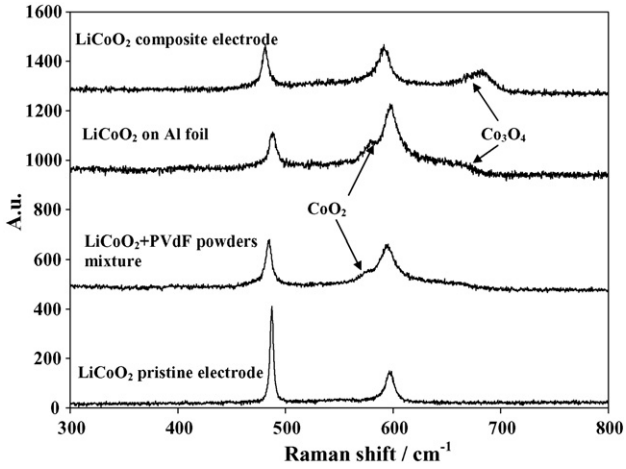

Fig. 2. Raman spectra of $LiCoO_2$ electrodes with/without PVdF binder after being stored for 2 weeks at 60 °C in standard electrolyte solutions: 1 M $LiPF_6$ in EC/EMC, $LiCoO_2$ powder that was stored in a similar solution that also contained PVdF powder, and a pristine $LiCoO_2$ electrode.

revealed that $LiCoO_2$ can catalyze the decomposition of the alkyl carbonates to form CO_2. This may involve the reduction of Co^{3+} to Co^{2+} ions that may easily dissolve in solutions. Hence, we can conclude that the following reactions take place:

$$4LiCoO_2 \xrightarrow{\text{disproportionation}} CoO_2 + Co^{II}Co_2^{III}O_4 + 2Li_2O,$$

$$Li_2O \xrightarrow{2HF} 2LiF + H_2O.$$

This reaction is driven by the presence of HF that reacts with Li_2O to form highly stable LiF and H_2O. The latter reacts with $LiPF_6$, thus forming more HF; hence, the reaction above is somewhat autocatalytic.

$LiPF_6$ undergoes thermal decomposition to LiF and PF_5, the latter reacting with trace water to form PF_3O and 2HF. It should be noted that LiF films are highly resistive [30]. The increasing impedance measured for $LiCoO_2$ electrodes upon storage in $LiPF_6$ solutions is attributed to the formation of LiF films. FTIR spectra of $LiCoO_2$ electrodes showed that pristine powder always contains surface Li_2CO_3, while $LiCoO_2$ stored in alkyl carbonate solutions contains surface species with alkyl carbonate groups ($ROCO_2Li$ or $(ROCO)_2Co$) [14]. We assume that such compounds can be formed by nucleophilic reactions between surface oxygen ions and alkyl carbonate molecules, which are very electrophilic. $LiCoO_2$ can be stabilized, even at elevated temperatures up to 90 °C, in acidic $LiPF_6$ solutions containing Co^{2+} ions (>100 ppm) [31]. Surfaces studied by XPS show that surface CoF_2 is formed, and thus inhibits detrimental Co^{2+} dissolution, surface Co_3O_4 formation, and a nucleophilic reaction between oxygen and alkyl carbonates on the $LiCoO_2$ surface. However, it should be noted that any presence of cobalt ions in solutions leads to the precipitation of cobalt compounds and metal on the negative electrode. Such precipitation may be detrimental to the passivation of Li-carbon negative electrodes [32]. Thus, Co-ion dissolution should be considered as a phenomenon to be avoided.

An obvious conclusion from the preceding results is that in the above reactions with HF, the formation of surface Co_3O_4 and the dissolution of Co ions occur mostly at the contact points between the $LiCoO_2$ particles and PVdF. These contact points are probably preferred sites for HF/H_2O adsorption to the electrode's surface, which then drives the above-described heterogeneous reactions. It should be noted that a similar detrimental effect of acidic $LiPF_6$ solutions was found for V_2O_5 electrodes [20]. The cycleability and kinetics of V_2O_5 in non-acidic, alkyl carbonate solutions (e.g., when the Li salt was $LiClO_4$) were very good. Conversely, their kinetics in acidic $LiPF_6$ solutions, especially at a low ratio between the active mass and solution volume, was very sluggish due to the formation of surface LiF [20]. To date we have not studied the possible dissolution of vanadium ions from V_2O_5 in solution, but we anticipate that the use of carbon-coated V_2O_5 (see Section 2) will lessen the detrimental effect of acidic species in solutions. The study of this material only began recently [22] and is now in progress.

The high sensitivity of $LiMO_2$ cathode materials to acidic species in solutions at elevated temperatures can be largely avoided by covering the particles of the active mass with a thin interphase layer of a basic species such as MgO. It was clearly demonstrated that $LiMn_2O_4$ (micro) particles covered by thin layers of MgO nanoparticles show high stability and low impedance in $LiPF_6$ solutions containing acidic contaminants, at 60 °C [33].

3.3. On $LiMn_{1.5}Ni_{0.5}O_4$ and $LiMn_{0.5}Ni_{0.5}O_2$ electrodes

As demonstrated in previous publications [17], $LiMn_{1.5}Ni_{0.5}O_4$ electrodes are remarkably stable in $LiPF_6$ solutions (1.5 M) of alkyl carbonates even at 60 °C, despite the fact that their redox activity is between 4.5 and 4.8 V (Li/Li^+) due to the $Ni^{2+}/Ni^{3+}/Ni^{4+}$ couples [34]. Impedance spectra indicate the development of highly stable surface films that protect the $LiMn_{1.5}Ni_{0.5}O_4$ electrodes from detrimental reactions with solution species, and inhibit any pronounced oxidation of the alkyl carbonate solvents. The formation of such films is especially evident at elevated temperatures. To date, we have not deciphered the structure of the surface films that are probably formed on $LiMn_{1.5}Ni_{0.5}O_4$.

We report herein on the highly stable behavior of $LiMn_{1.5}Ni_{0.5}O_4$ electrodes, prepared from both micro- and nanoparticles (≈20 nm in size, produced by SCR [19]) of the active material. Fig. 3 compares their Raman spectra stored at 70 °C in $LiPF_6$ solutions, to those of pristine powders. These spectra demonstrate very clearly the remarkable stability of these nano- and microparticulate materials. As expected for the smaller sized particles, the peaks in the spectra of the nano-materials are broader. Fig. 4 shows some aspects related to the performance of the electrodes comprising nanoparticles of $LiMn_{1.5}Ni_{0.5}O_4$. The regular CV curves of these electrodes clearly reflect the two reversible Ni^{2+}/N^{3+}, Ni^{3+}/Ni^{4+} couples. In contrast, electrodes comprising nanoparticles that were aged in solution for a few weeks show nearly featureless voltammograms, which reflect very sluggish kinetics (marked in Fig. 4). However, when the same aged material was ground with carbon black and the composite electrode was prepared from the ground material, its CV reflects fast kinetics and is very similar to that of a pristine electrode, as demonstrated in Fig. 4. These results show that the deactivation of the $LiMn_{1.5}Ni_{0.5}O_4$ nanoparticles due to aging is only a superficial phenomenon related to surface films that interfere badly with the electrical contact of the particles and charge transfer to/from them. The bulk of the active mass was not affected by aging. This demonstrates the stability of this material. The rate capability of this material is

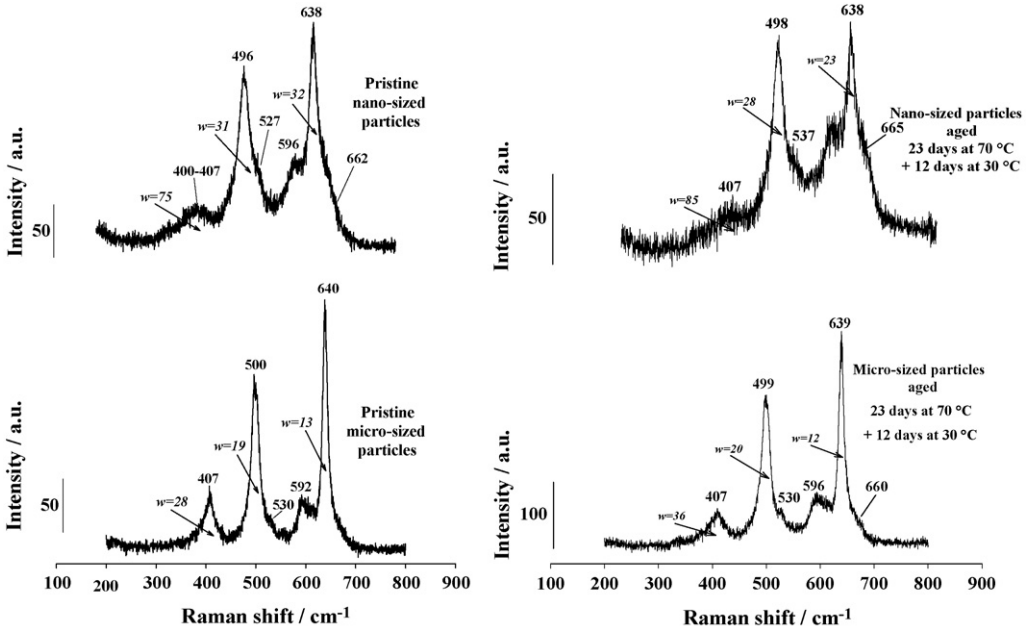

Fig. 3. Raman spectra of micro- and nano-sized $LiNi_{0.5}Mn_{1.5}O_4$ pristine material and material aged (70 °C) in DMC-EC (2:1)/1.5 M $LiPF_6$ solutions, as indicated. The main peak positions and the corresponding FWHM values are also marked.

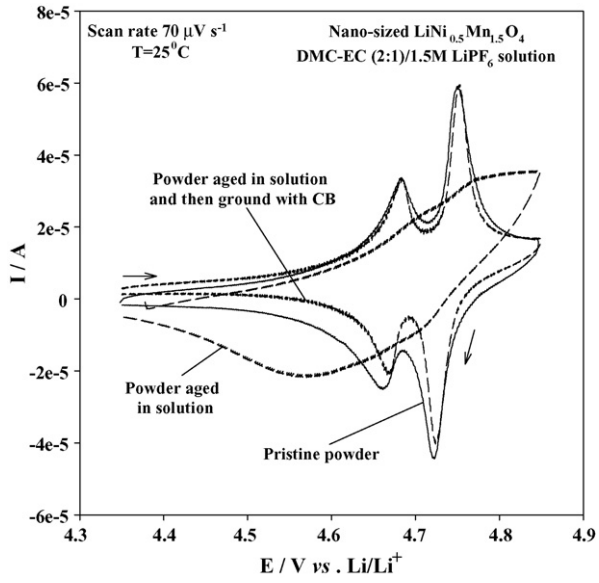

Fig. 4. Cyclic voltammograms (CVs) of thin electrodes (on Al foil current collectors) comprising nano-sized particles of the pristine $LiNi_{0.5}Mn_{1.5}O_4$ powder, of a powder aged in a DMC-EC (2:1)/1.5 M $LiPF_6$ solution at $T = 30\,^{\circ}C$ for 35 days, and of the same aged powder ground with carbon black (15%). All the electrodes were free of PVdF binder. CVs were recorded in DMC-EC (2:1)/1.5 M $LiPF_6$ solutions at $T = 25\,^{\circ}C$ using three-electrode flooded cells, at the potential scan rate of $70\,\mu V\,s^{-1}$.

also impressive. Up to 1*C* rates, the maximal practical capacity (around $140\,mAh\,g^{-1}$) could be obtained. About 80% of that capacity can be obtained at 5*C* rates. Impedance spectroscopy of electrodes comprising nanoparticles of $LiMn_{1.5}Ni_{0.5}O_4$ indicates that up to 70 °C (the upper temperature that we have studied so far), the surface chemistry develops stable, passivating surface films as the temperature increases. In other words, surface films formed at high temperatures remain stable and do not change at lower temperatures, as was found for electrodes comprising $LiMn_{1.5}Ni_{0.5}O_4$ microparticles [17]. This is reflected by the fact that once an electrode is exposed to an elevated temperature, its impedance behavior at this temperature does not change, even after prolonged storage/cycling of the electrodes at a lower temperature. It should also be noted that some Mn and Ni ion dissolution from these electrodes could be detected only after prolonged (several weeks) storage at 60 °C.

We also prepared nanoparticles of $LiMn_{0.5}Ni_{0.5}O_2$ by the SCR method. Fig. 5 compares the slow scanning rate CV of a composite electrode comprising nanoparticles of $LiMn_{0.5}Ni_{0.5}O_2$ that was aged at 60 °C in an EC-DMC/$LiPF_6$ solution, to that of the same pristine electrode. This comparison demonstrates the relatively high practical capacity of this material of close to $200\,mAh\,g^{-1}$; and its high stability during cycling and aging even at elevated temperatures. The high stability of both $LiMn_{1.5}Ni_{0.5}O_4$ and $LiMn_{0.5}Ni_{0.5}O_2$ is striking when compared to that of $LiMn_2O_4$ (spinel structure) electrodes at elevated temperatures. The latter materials are well known for their instability at elevated temperatures, reflected by accelerated capacity fading upon cycling and pronounced Mn ion dissolution (which leads to the destruction and deactivation of the active mass) [35]. Hence, it appears that the

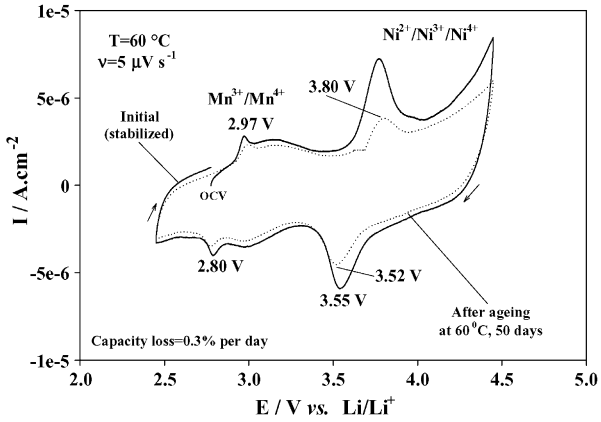

Fig. 5. Slow scan rate voltammograms of composite electrodes comprising nano-$LiNi_{0.5}Mn_{0.5}O_2$ at the initial (steady) state and after 50 days of ageing in solution at 60 °C. Three-electrode coin-type cells, DMC-EC (2:1)/1.5 M $LiPF_6$ solution.

replacement of part of the Mn ions by Ni ions in these materials stabilizes them. One reason may relate to the different oxidation state of Mn in the two compounds. The $Mn^{3.5+}$ oxidation state in the $LiMn_2O_4$ spinel, means that some Mn is in the oxidation state 3+ and this makes it prone to disproportionation $Mn^{III} \rightarrow Mn^{II} + Mn^{IV}$. It is well known that it is the Mn^{II} that is subject to dissolution. In contrast, the oxidation state of Mn in $LiMn_{1.5}Ni_{0.5}O_4$ is higher and hence it cannot proportionate to form soluble Mn^{II} ions. Beyond that, our hypothesis, which has

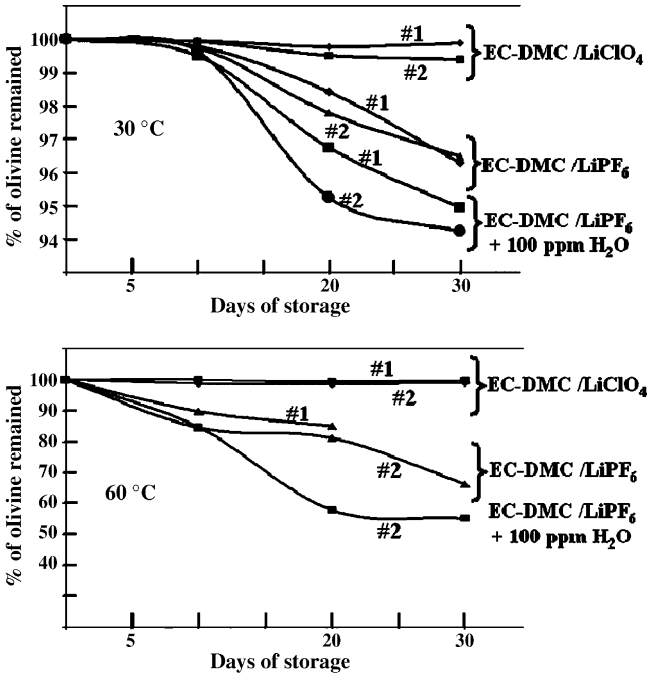

Fig. 6. Results of Fe ion dissolution tests from $LiFeO_4$ olivine powders at 30 °C (top) and 60 °C (bottom) in three solutions: $LiClO_4$ 1 M in EC/DMC = 1:1, $LiPF_6$ 1 M in EC/DMC, and $LiPF_6$ 1 M = 1:1 in EC/DMC = 1:1 with 100 ppm of H_2O. Sample #1: Produced by reacting Li_3PO_4, H_3PO_4, and $3FeC_6H_5O{\cdot}2H_2O$ (see Section 2). The final product contains 3% carbon. Sample #2: Produced by reacting $FeC_2O_4{\cdot}2H_2O$, $NH_4H_2PO_4$, and 0.5 Li_2CO_3 (see Section 2). The final product contains 3% C, surface FeP, and/or Fe_2P. The results are expressed in percent of compound remaining (based on the calculation of %Fe dissolved).

to be proven (work in progress), is that the presence of Ni in the lattice makes the oxygen atoms more nucleophilic. Thus, surface oxygen ions nucleophilically attack the electrophilic alkyl carbonate molecules that forms protective surface films comprising ROLi and $ROCO_2Li$ species, which behave according to the SEI model [16], thus protecting the active mass and preventing transition metal dissolution, but allowing Li-ion transport through them. This hypothesis is partially supported by previous studies that showed that $LiNiO_2$ is much more reactive to alkyl carbonate solutions than both $LiMn_2O_4$ and $LiCoO_2$ FTIR studies of $LiNiO_2$ powder/electrodes clearly reflected the formation of surface $ROCO_2Li$ compounds on this material [36].

3.4. On $LiFePO_4$ electrodes

Three $LiFePO_4$ samples were synthesized as described above in Section 2. The synthesis routes were varied to produce $LiFePO_4$ from a sol–gel method (Sample 1); a solid-state processing method (Sample 2); and a hydrothermal method (Sample 3).

Fig. 6 shows the results of storage tests for two representative samples at 30 and 60 °C in an EC-DMC/1 M $LiClO_4$ (non-acidic) solution, an EC-DMC/$LiPF_6$, and an EC-DMC/$LiPF_6$ solution contaminated with water (100 ppm). The latter two solutions contain HF, and hence, should be considered as acidic. During 30 days of storage, solution samples were taken out and examined by ICP. From the iron content in these samples, it was possible to follow Fe ion dissolution upon storage, and hence, to calculate the loss in the active mass as a function of storage time, temperature, and solution composition. The results displayed in Fig. 6 reveal the following findings:

1. In the $LiClO_4$ solution, which does not contain acidic contaminants, Fe ion dissolution and the consequent loss of the active mass is negligible even at elevated temperatures.
2. As the solution becomes more acidic (i.e., solutions containing $LiPF_6$ as the salt and those further contaminated by water), the dissolution of Fe ions becomes more pronounced.
3. As expected, higher temperatures lead to more pronounced Fe ion dissolution.
4. The materials containing a higher percentage of intrinsic carbon (e.g., 3% *versus* <2%) and which are not contaminated by other phases other than $LiFePO_4$ are the most stable in all three solutions studied.

Based on these data, Fig. 7 presents the voltammetric and impedance behavior of electrodes comprising the *most* stable olivine material: namely Sample 1 produced by sol–gel methods that result in about 3% carbon inclusion, in combination with the non-acidic solution ($LiClO_4$). Fig. 7a compares the steady state, slow scanning rate voltammograms of these electrodes measured after two different periods of storage at 30 °C (10 and 20

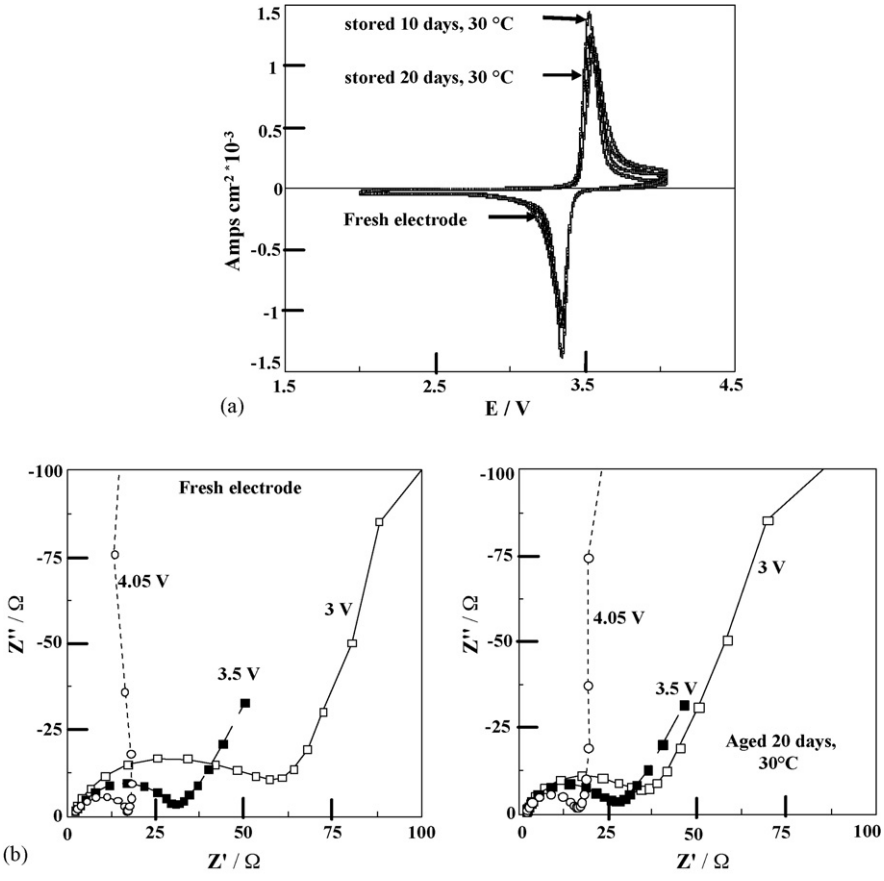

Fig. 7. Typical stable behavior of a $LiFeO_4$ olivine electrode in solutions containing no acidic contamination, e.g., in $LiClO_4$ 1 M EC/DMC = 1:1. The active mass was prepared from Li_3PO_4, H_3PO_4, and $FeC_6H_5O_7{\cdot}2H_2O$ (Sample #1, see Section 2). CV (a) and EIS (b) of fresh and aged electrodes are presented.

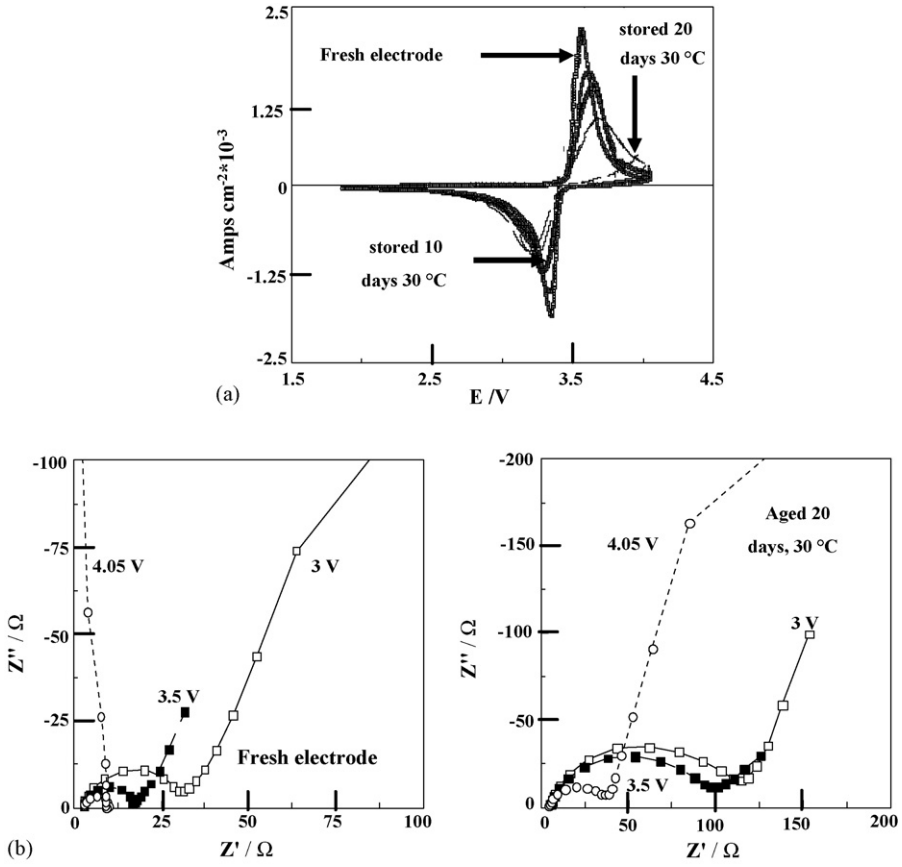

Fig. 8. Typical unstable behavior of a $LiFeO_4$ olivine electrode in solutions containing acidic contamination, e.g., in $LiPF_6$ 1 M EC/DMC = 1:1. The active mass was prepared from $FeC_2O_4{\cdot}2H_2O$, $NH_4H_2PO_4$, and 0.5 Li_2CO_5 (Sample #2, see Section 2). CV (a) and EIS (b) of fresh and aged electrodes are presented.

days, as indicated) to that of the pristine electrode. All the three CVs in the figure are nearly identical and reflect the expected capacity of close to 150 mAh g^{-1}. Fig. 7b compares families of Nyquist plots obtained from these electrodes in $LiClO_4$ solution at different potentials soon after stabilization (i.e., after the electrode underwent the first few voltammetric cycles in the 2.5–4 V range *versus* Li/Li^+); and after storage for 20 days in solution. The impedance behavior of these electrodes is very interesting. It decreases during the course of delithiation as the electrode's potential increases. At potentials in which the electrode is fully delithiated (e.g., >4 V *versus* Li/Li^+), the Nyquist plots comprise a semicircle and a straight line at nearly 90°. These spectra portray the interfacial charge transfer coupled with interfacial capacitance at high frequency, and the pure capacitive behavior at low frequency. This reflects the smooth delithiation of these electrodes and the absence of side reactions. Further analysis of the impedance behavior of these systems is beyond the scope of the present paper. That storage leaves the impedance spectra of this system *nearly invariant* is particularly remarkable (Fig. 7b). Hence, the data presented in Fig. 7 correlate very well with that presented in Fig. 6 and demonstrate the highly stable behavior of these systems.

Fig. 8 shows similar data as in Fig. 7, but for a less stable material/solvent combination, namely Sample #2 ("solid-state" $LiFePO_4$) in $LiPF_6$ solution. The CVs in Fig. 8a display a slight decrease in the electrode's capacity upon storage. The Nyquist plots in Fig. 8b reflect the increase in the electrode's impedance. Combined, these results show that in addition to Fe ion dissolution (and hence to a loss in the active mass), storage in $LiPF_6$ solutions leads to the precipitation of resistive surface films that make the kinetics of the electrodes to be more sluggish. We assume that the presence of HF has a doubly detrimental effect: Fe ions can be exchanged by protons, and the Li ions in the lattice near the surface react with F^- ions, thus forming surface LiF. Surface films comprising LiF are known to be highly resistive to Li-ion migration [30].

The exact mechanism of Fe dissolution, the impact of HF and H_2O contaminants on enhanced Fe ion dissolution, and the surface chemistry of $LiFePO_4$ electrodes in these solutions has not yet been determined. The relevant research work is in progress.

4. Conclusions

All commonly-used cathode materials develop rich surface chemistry in alkyl carbonate solutions. This includes acid–base reactions, nucleophilic reactions, induced polymerization, and transition metal dissolution that is accompanied by phase transitions.

Examples of the formation of surface films are:

- All cathodes—LiF, $ROCO_2Li$, $ROCO_2M$, ROLi, MCO_3, Li_2CO_3, MF_2 (M = transition metal), polycarbonates;

- $Li[Mn,Ni]O_4 \rightarrow \lambda$-$MnO_2$;
- $LiCoO_2 \rightarrow Co_3O_4$;
- Li_xMnO_2 (layered materials) → surface $LiMn_2O_4$ spinel.

Co^{III} ions can oxidize alkyl carbonates to CO_2, thus forming Co^{II} ions that easily dissolve. On the one hand, the presence of Co^{II} ions in solutions stabilizes $LiCoO_2$ at high temperature (even >80 °C). However, in general, the deposition of transition metal compounds on all negative carbon electrodes may be detrimental to their passivation. The most detrimental conditions for capacity fading of all cathode materials are acidic solutions: those employing $LiPF_6$, especially in wet, high solution/electrode mass ratios. The contact points with the binder are the most active in terms of active mass corrosion. Corrosion can be prevented by basic interphase or the use of acid scavengers additives in solutions. Finally, electrodes comprising nano-$LiMn_{0.5}Ni_{0.5}O_2$ and $LiMn_{1.5}Ni_{0.5}O_4$ show high stability up to 5 V in alkyl carbonates/$LiPF_6$ solutions (even >60 °C). In the case of $LiFePO_4$ electrodes, optimum stability is derived from carbon inclusion/coating of the active material and the use of non-acidic electrolyte solutions such as EC-DMC/1 M $LiClO_4$. Quite remarkably, these electrode assemblies can be stored for long periods of time even at elevated temperature without showing marked changes in their impedance spectra.

References

[1] G. Amatucci, J.M. Tarascon, J. Electrochem. Soc. 149 K (2002) 31.

[2] A.K. Padhi, K.S. Nanjundaswamy, J.B. Goodenough, J. Electrochem. Soc. 144 (1997) 1188–1194;
A.S. Anderson, B. Kalska, L. Haggstrom, J.O. Thomas, Solid State Ionics 130 (2000) 41;
A. Yamada, S.C. Chung, K. Hinokuma, J. Electrochem. Soc. 148 (2001) A224.

[3] T. Ohzuku, Y. Makimura, Chem. Lett. 30 (2001) 642–643;
X. Wu, S.H. Chang, Y.H. Park, K.S. Ryu, J. Power Sources 137 (2004) 105–110;
Y. Sun, Y. Xia, H. Noguchi, Electrochem. Solid State Lett. 8 (2005) A637–A640.

[4] M.E. Spahr, P. Novak, B. Schnyder, O. Haas, R. Nespe, J. Electrochem. Soc. 145 (1998) 1113;
Z. Lu, D.D. MacNeil, J.R. Dahn, Electrochem. Solid State Lett. 4 (2001) A191;
T. Ohzuku, Y. Makimura, Chem. Lett. 30 (2001) 744.

[5] K. Dokko, M. Mohamedi, N. Anzue, T. Itoh, I. Uchida, J. Mater. Chem. 12 (2002) 3688;
K. Sun, K.-J. Hong, J. Prakash, K. Amine, Electrochem. Commun. 4 (2002) 344;
D. Aurbach, B. Markovsky, Y. Talyossef, G. Salitra, H.-J. Kim, S. Choi, J. Power Sources, (2006) in press.

[6] C. Delmas, I. Saadoune, Solid State Ionics 370 (1992) 53–56;
R. Alcantara, P. Lavela, J.L. Tirado, E. Zhecheva, R. Stoyanova, J. Solid State Electrochem. 3 (1999) 121.

[7] J.O. Besenhard (Ed.), Handbook of Battery Materials, Wiley-VCH, Weinheim, NY, Toronto, 1999, pp. 304–314.

[8] M. Morcrette, P. Rozier, L. Dupont, E. Mugnier, L. Sannier, J. Galy, J.M. Tarascon, Nat. Mater. 2 (2003) 755–761.

[9] P. Novak, J.-C. Panitz, F. Joho, M. Lanz, R. Imhof, M. Coluccia, J. Power Sources 90 (2000) 52–58.

[10] M. Balasubramanian, X. Sun, X.Q. Yang, J. McBreen, J. Power Sources 92 (2001) 1–8.

[11] Y. Teradaa, K. Yasakaa, F. Nishikawab, T. Konishic, M. Yoshiod, I. Nakaia, J. Solid State Chem. 156 (2001) 286–291.

[12] Y.S. Meng, G. Ceder, C.P. Grey, W.-S. Yoon, Y. Shao-Horn, Electrochem. Solid State Lett. 7 (2004) A155–A158.

[13] C.P. Grey, N. Dupré, Chem. Rev. 104 (2004) 4493–4512.

[14] D. Aurbach, B. Markovsky, M.D. Levi, E. Levi, A. Schechter, M. Moshkovich, Y. Cohen, J. Power Sources 95 (1999) 81–82.

[15] D. Aurbach, J. Power Sources 89 (2000) 206.

[16] E. Peled, D. Golodnitsky, J. Penciner, in: J.O. Besenhard (Ed.), Handbook of Battery Materials, Wiley-VCH, Weinheim, NY, Toronto, 1999, pp. 419–453 (Part 3, Chapter 6).

[17] B. Markovsky, Y. Talyossef, G. Salitra, D. Aurbach, H.-J. Kim, S. Choi, Electrochem. Commun. 6 (2004) 821–826.

[18] W.-S. Yoon, M. Balasubramanian, X.Q. Yang, Z. Fu, D.A. Fisher, J. McBreen, J. Electrochem. Soc. 151 (2004) A246.

[19] M.G. Lazarraga, L. Paskual, H. Gadjov, D. Kovacheva, K. Petrov, J.M. Amarilla, R.M. Rojas, M.A. Martin-Luengo, J.M. Rojo, J. Mater. Chem. 14 (2004) 1640.

[20] Y.S. Cohen, D. Aurbach, Electrochem. Commun. 6 (2004) 536–542.

[21] S.V. Pol, A. Gedanken, Chem. Eur. J. 10 (2004) 4467.

[22] A. Odani, V.G. Pol, M. Koltypin, A. Gedanken, D. Aurbach, Adv. Mater. 18 (2006) 1431.

[23] J.S. Gnanaraj, Y.S. Cohen, M.D. Levi, D. Aurbach, J. Electroanal. Chem. 516 (2001) 89.

[24] D. Aurbach, Y. Goffer, in: D. Aurbach (Ed.), Nonaqueous Electrochemistry, Marcel Dekker Inc., NY, 1999 (Chapter 4).

[25] K. Kanamura, J. Power Sources 123 (1999) 81–82.

[26] H. Ohno (Ed.), Electrochemical Aspects of Ionic Liquids, John Wiley & Sons Inc., 2005.

[27] B. Garcia, S. Lavallée, G. Perron, C. Michot, M. Armand, Electrochim. Acta 49 (2004) 4583–4588.

[28] M. Moshkovich, M. Cojocaru, H.E. Gottlieb, D. Aurbach, J. Electroanal. Chem. 497 (2001) 84–96.

[29] E. Markevich, G. Salitra, D. Aurbach, Electrochem. Commun. 7 (2005) 1298.

[30] D. Aurbach, E. Zinigrad, A. Zaban, J. Phys. Chem. 100 (1996) 3089.

[31] D. Aurbach, B. Markovsky, A. Rodkin, Y. Talyossef, G. Salitra, H.-J. Kim, J. Electrochem. Soc. 151 (2004) A1068–A1076.

[32] N. Kumagai, S. Komaba, Y. Kataoka, M. Koyanagi, Chem. Lett. N10 (2000) 1154;
S. Komaba, N. Kumagai, Y. Kataoka, Electrochim. Acta 47 (2002) 1229.

[33] J.S. Gnanaraj, V.G. Pol, A. Gedanken, D. Aurbach, Electrochem. Commun. 5 (2003) 940.

[34] Y. Terada, K. Yasaka, F. Nishikawa, T. Konishi, M. Yoshio, I. Nakai, J. Solid State Chem. 156 (2001) 286.

[35] D. Guyomard, J.M. Tarascon, J. Electrochem. Soc. 140 (1993) 3071–3081.

[36] D. Aurbach, K. Gamolsky, B. Markovsky, G. Salitra, Y. Gofer, J. Electrochem. Soc. 147 (2000) 1322.